water

MDPI

Article

Photocatalytic Degradation of Algal Organic Matter Using TiO_2/UV and Persulfate/UV

Luan de Souza Leite [1,*], Maria Teresa Hoffmann [1], Danilo Vitorino dos Santos [2] and Luiz Antonio Daniel [1]

[1] Department of Hydraulics and Sanitation, São Carlos School of Engineering, University of São Paulo, São Carlos 13566-590, Brazil
[2] School of Pharmaceuticals Sciences of Ribeirão Preto, University of São Paulo, Ribeirão Preto 14040-900, Brazil
* Correspondence: luanleite@usp.br

Abstract: Eutrophication in water reservoirs releases algal organic matter (AOM), a key precursor to the formation of disinfection by-products (DBPs) during the disinfection process. Typical drinking water treatment is not efficient for AOM removal, and advanced treatments are necessary for the removal of residual AOM before chlorination. UV-based technology with PS and TiO_2 is widely used as a pre-oxidation step in water treatment; however, no publications have focused on them for AOM degradation. In this context, this work investigated the effect of oxidant concentration (0.1 to 0.5 $g{\cdot}L^{-1}$) and pH (6 to 10) on AOM degradation with TiO_2/UV and persulfate (PS)/UV using response surface methodology. In general, PS/UV was more effective in removing protein, while TiO_2/UV was more effective in carbohydrate degradation. TiO_2/UV removals varied from 27 to 57% for protein and from 48 to 86% for carbohydrates. The optimal condition (57% for protein and 86% for carbohydrates) was obtained using 0.5 $g{\cdot}L^{-1}$ TiO_2 at pH 10. PS/UV removals varied from 33 to 81% for protein and from 24 to 53% for carbohydrates. The optimal condition (81% for protein and 53% for carbohydrates) was obtained using 0.5 $g{\cdot}L^{-1}$ PS concentration at pH 8. Degradation kinetics showed a good fit to the pseudo-first-order model (R^2 > 95%) for both processes. The DBP formation reductions observed with TiO_2/UV—trihalomethane (THM) (85 to 86%) and chloral hydrate (CH) (94 to 96%)—were similar to the efficiencies observed for PS/UV—THM (87 to 89%) and CH (83 to 88%). These results show the efficiency of UV-based technology for AOM degradation and the control of DBP formation.

Keywords: algal organic matter; algae oxidation; natural organic matter; DBP control

Citation: Leite, L.d.S.; Hoffmann, M.T.; dos Santos, D.V.; Daniel, L.A. Photocatalytic Degradation of Algal Organic Matter Using TiO_2/UV and Persulfate/UV. *Water* **2024**, *16*, 1626. https://doi.org/10.3390/w16111626

Academic Editors: Gongduan Fan, Kaiqin Xu and Banghao Du

Received: 7 May 2024
Revised: 29 May 2024
Accepted: 5 June 2024
Published: 6 June 2024

1. Introduction

Algal blooms in drinking water supplies have been a significant challenge for water treatment [1]. Global warming and high nutrient loads can intensify this phenomenon in the future, making it a more serious problem [2]. Algal organic matter (AOM) is released during algae growth through metabolic processes or cell lysis, and it is composed mainly of carbohydrates and proteins [3]. AOM can impact directly the final water quality because it is a major precursor of disinfection by-products (DBPs), such as trihalomethanes (THMs) and chloral hydrates (CHs), during chlorination [4].

The typical processes used for drinking water treatment (conventionally coagulation–flotation or sedimentation and sand filtration) are not efficient for AOM removal (less than 70%). For example, Henderson et al. (2010) [5] used coagulation with aluminum sulphate and dissolved air flotation for AOM removal, finding efficiencies ranging 46 from 71%. Sedimentation removal varied from 25 to 57% using typical coagulants, such as aluminum sulfate and ferric chloride [6,7]. It is important to mention that these results were found in the laboratory under optimal conditions that usually do not occur in real water matrices and drinking water facilities. No information is available in the literature about AOM removal via rapid sand filtration. Nevertheless, low removals are expected as dissolved organic

carbon (DOC) removals ranging from 12 to 33% were reported in slow sand filtration in water treatment facilities [8]. Thus, advanced treatments are needed for the removal of residual AOM before the chlorination step to avoid DBP formation.

The implementation of pre-oxidation processes before the coagulation process can be a suitable approach to improve AOM removal. Oxidizing agents like ozone (O_3), chlorine, or potassium permanganate ($KMnO_4$) can break down complex organic molecules into smaller, more easily coagulable fragments, thereby reducing the amount of coagulant needed and increasing the coagulation efficiency [9,10]. Naceradska et al. (2017) [11] observed that $KMnO_4$ pre-oxidation (0.8–4.8 mg $KMnO_4 \cdot L^{-1}$) of *Microcystis aeruginosa* AOM increased removal by 5–12%. Novotná et al. (2020) [12] applied O_3 (0.05–4.0 mg$\cdot L^{-1}$) as the pre-oxidation of the non-proteinaceous fraction of *Chlorella vulgaris* AOM and ozonation increased the coagulation efficiency up to 7%. Furthermore, pre-oxidation can also improve AOM adsorption when an activated carbon filter is applied downstream to the coagulation [13]. Therefore, pre-oxidation stands out as a process that can be used to improve AOM removal in water treatment.

The available literature about this topic was collected on Scopus using "algal organic matter" and "oxidation" as the keywords (with the following Boolean descriptors: "algal organic matter" AND "oxidation"). Afterwards, manual screening was conducted, considering two criteria for data selection: peer-reviewed articles with new data in English and studies performed without microalgae cell presence. Then, 15 articles were selected as references for the discussion. The oxidizing agents reported for AOM degradation are ultraviolet (UV) [14,15], O_3 [12,16], $KMnO_4$ [11], potassium persulfate (PS), peroxydisulfate [17], hydrogen peroxide (H_2O_2) [18], and ferrate (Fe(VI)) [19]. The oxidation processes showed low and moderate efficiencies for AOM removal (0–67%) from water, and the results were reported in terms of the removal of dissolved (DOC) or total organic carbon. UV-based oxidative processes are the most studied and applied at full-scale due to the easily installation and operation of a UV unit with a disinfection efficiency for a variety of microorganisms [20]. UV is not effective for AOM degradation when applied alone [14,15] and is therefore usually used together with another oxidant. Different combinations were reported in the literature, such as H_2O_2/UV [21], permonosulfate/UV [22], UV/H_2O_2/O_3 [23], O_3/UV [24], Fenton [18], and photo-Fenton [18].

UV-based technology with PS and TiO_2 is widely applied for the removal of microalgae cells, micropollutants, and natural organic matter from water [25,26]. TiO_2 is the most common photocatalyst because it is effective for a wide range of contaminants, environmental safety, photochemical stability at a wide pH range, and is relatively cheap [27]. PS is also a popular oxidant due to its benefits, such as cost effectiveness, stability during transportation and storage, and generation of non-toxic by-products [28]. These oxidants can be scaled up to accommodate varying treatment capacities, making them suitable for both small-scale and large-scale applications. Despite the advantages mentioned, there have been no studies published to date focusing on them for AOM degradation with TiO_2/UV and PS/UV. Based on this, this work investigated the AOM removal process from *Chlorella sorokiniana* with TiO_2/UV and PS/UV using protein and carbohydrate analysis. The goals of this study were as follows: (1) to optimize these processes using response surface methodology; (2) to assess the kinetics of AOM oxidation; and (3) to evaluate DBP formation before and after oxidation.

2. Materials and Methods

2.1. AOM Extraction

Chlorella sorokiniana 211–8 k was obtained from Culture Collection of Algae and Protozoa (Argyll, Scotland) and cultivated using the protocol described by Leite et al. (2021) [29]. The cells were harvested at the stationary growth phase, which occurred after seven days of cultivation. The collected suspension was then centrifuged at 1500× *g* for 10 min), washed twice with ultrapure water, and frozen at −20 °C for further processing.

The AOM from *Chlorella sorokiniana* cells was extracted using the method described by Leite et al. (2019) [30]. The process involved resuspending the cells in ultrapure water, followed by two cycles of ultrasonication on ice. The resulting suspension was then centrifuged at 1500× *g* for 10 min, and the supernatant was filtered through a 0.45 µm membrane. The extracted AOM was stored at −20 °C until further analysis. The dissolved organic carbon (DOC) content of the AOM was determined using a TOC-L analyzer (Shimadzu, Kyoto, Japan).

2.2. Photocatalytic Oxidation Experiments

The performance of TiO_2/UV and PS/UV for AOM removal was evaluated via protein and carbohydrate analysis. Protein concentrations were measured using the Bradford reagent (Sigma-Aldrich, St. Louis, MO, USA) at a wavelength of 595 nm. Bovine serum albumin (Sigma-Aldrich, USA) was used as the standard reference. Total carbohydrate content was quantified using the phenol-sulfuric acid method [31] at 488 nm. Glucose (Qhemis, Jundiaí, Brazil) was used as a standard. Each analysis was performed in triplicate.

Test water was prepared by mixing ultrapure water with an AOM concentration of 5 mg DOC·L^{-1}, total alkalinity of 25 mg $CaCO_3$·L^{-1} (utilizing 8.5 g Na_2HCO_3·L^{-1} solution). The pH was adjusted at pH 8. This composition reflects the typical water quality usually found in the environment [6,29]. Despite the AOM being dosed by DOC, it was not used as a parameter here because the PS amount used in the test can interfere with its quantification.

The experiments were performed in a collimator device, which applied a low-pressure mercury UV lamp (maximum 15 W) with a specific wavelength of 254 nm. The power density of the UV dose used in this study was measured as 0.658 mW·cm^{-2}. The 50 mL test water was placed in a beaker (internal diameter of 6.7 cm, external diameter of 7.0 cm, and height of 3.2 cm) which resulted in a sample layer of 1.5 cm. The lamp was turned on 10 min before the tests.

An appropriate amount of PS/TiO_2 was added to the samples, and the beakers were carefully placed inside the collimator device. Next, the samples were continuously mixed at 80 rpm using a magnetic stirrer. A bulk solution of potassium persulfate (Sigma-Aldrich, USA) was prepared in ultrapure water. TiO_2 nanoparticles (Degussa P25®, Sigma-Aldrich, USA) were previously dried at 100 °C for 1 h to eliminate the water. The characterization of TiO_2 nanoparticles used can be found in a previous study [27]. Then, samples were collected at the end of each test and submitted to different processes before the protein and carbohydrate analysis. Samples from TiO_2 oxidation were filtered into 0.45 µm glass microfiber membranes (Macherey-Nagel, Düren, Germany) to remove the nanoparticles. Sodium thiosulfate solution (Synth, Diadema, Brazil) was added to the solution after the PS/UV process at a mass ratio of 1.2:1 to neutralize residual PS. Preliminary tests were carried out to ensure these processes did not affect the spectrometric quantification of carbohydrates and proteins. Blank tests were performed with ultrapure water and test water without oxidants to check their potential interference.

2.3. Response Surface Methodology

Response surface methodology was employed for the optimization of the PS/TiO_2 concentration (0.1 to 0.5 g·L^{-1}) and pH (6 to 10) on AOM degradation. These concentrations were selected based on preliminary results. The pH range selected is often found in water reservoirs [32]. Two variables (Table 1) were used and optimized using a central composite design, based on a three-factor level (−1, 0, +1) with face-centered alpha (a = 1). The experiment was carried out within 2 h, which represents a UV dose of 4.74 J·cm^{-2}. The data obtained were assessed by multiple regression and ANOVA using Minitab software (version 18.1, Minitab LLC., State College, PA, USA).

Table 1. The independent variables and their corresponding values for oxidation experiments.

Variables	Units	−1	0	1
pH	-	6	8	10
PS or TiO_2	$g{\cdot}L^{-1}$	0.1	0.3	0.5

2.4. Adsorption Tests

AOM adsorption with TiO_2 nanoparticles was quantified by DOC, protein, and carbohydrate analysis. The effect of pH (6, 8, and 10) was analyzed under continuous agitation at 80 rpm with 0.5 $g{\cdot}L^{-1}$ TiO_2 without UV light. After 2 h, samples were collected and filtered through 0.45 µm glass microfiber membranes (Macherey-Nagel, Germany) for nanoparticle removal.

The charges involved in the process were measured by zeta potential. The zeta potential of AOM and TiO_2 solutions over a wide pH range (2 to 11) was determined via Zetasizer Nano-ZS (Malvern, Malvern, UK) at 25 °C.

2.5. Kinetics

The optimal conditions for the TiO_2/UV and PS/UV processes for AOM degradation were found at different times (0.25 to 2.5 h). The UV doses tested varied from 0.59 (0.25 h) to 5.92 (2.5 h) $J{\cdot}cm^{-2}$. The results found were modelled using the pseudo-first-order model (Equation (1)).

$$\ln\left(\frac{C}{C_o}\right) = -k \times t \quad (1)$$

where C_o and C_t ($mg{\cdot}L^{-1}$) are the initial AOM concentration (5 mg $DOC{\cdot}L^{-1}$) and the concentration at time t (min), respectively. k is the reaction rate (h^{-1}).

Linear regression was used to assess the fit of the experimental data to the mathematical model (Equation (1)) using GraphPad Prism software (version 6.01, La Jolla, CA, USA). Model adjustment was analyzed by the coefficient of determination (R^2).

2.6. DBP Formation

The reduction in DBP formation was determined after the TiO_2/UV and PS/UV processes. Chlorination was performed according to a previous study [33]. Samples (10 mL) were collected from previous experiments (Section 2.4) and placed in amber glass bottles. Sodium hypochlorite (Sigma-Aldrich, USA) was added at a Cl_2:DOC mass ratio of 5:1. Then, the bottles were sealed and placed in a dark environment at a temperature of 20 °C.

After 7 days, free chlorine was quenched with ascorbic acid (Qhemis, Brazil) at a mass ratio of 6:1. The samples were promptly extracted using MTBE as a solvent (Sigma-Aldrich, USA). The concentrations of THM and CH were determined using gas chromatography spectrometry (CG-2010 Shimadzu, Japan) using the standard USEPA 551 method [34]. A mixed standard of EPA 501/601 Trihalomethanes Calibration Mix (Supelco, Sigma-Aldrich, Saint Louis, MO, USA), and CH (Dinâmica, Indaiatuba, São Paulo, Brazil) were used for the calibration method. Each condition was performed in duplicate.

Statistical analyses were carried out using GraphPad Prism software (version 6.01, USA) with a significance level set at 0.05.

3. Results

3.1. Response Surface of TiO_2

The effect of the TiO_2 concentration (0.1 to 0.5 $g{\cdot}L^{-1}$) and pH (6 to 10) on AOM degradation with TiO_2/UV is shown in Figure 1. Removals varied from 27.1 to 57.4% for protein (Figure 1a) and from 47.7 to 86.1% for carbohydrates (Figure 1b). The highest removals for protein (57.4%) and carbohydrates (86.1%) were obtained using a TiO_2 concentration of 0.5 $g{\cdot}L^{-1}$ at pH 10, while the lowest removals for protein (27.1%) and carbohydrates (47.7%) were found using a TiO_2 concentration of 0.1 $g{\cdot}L^{-1}$ at pH 8.

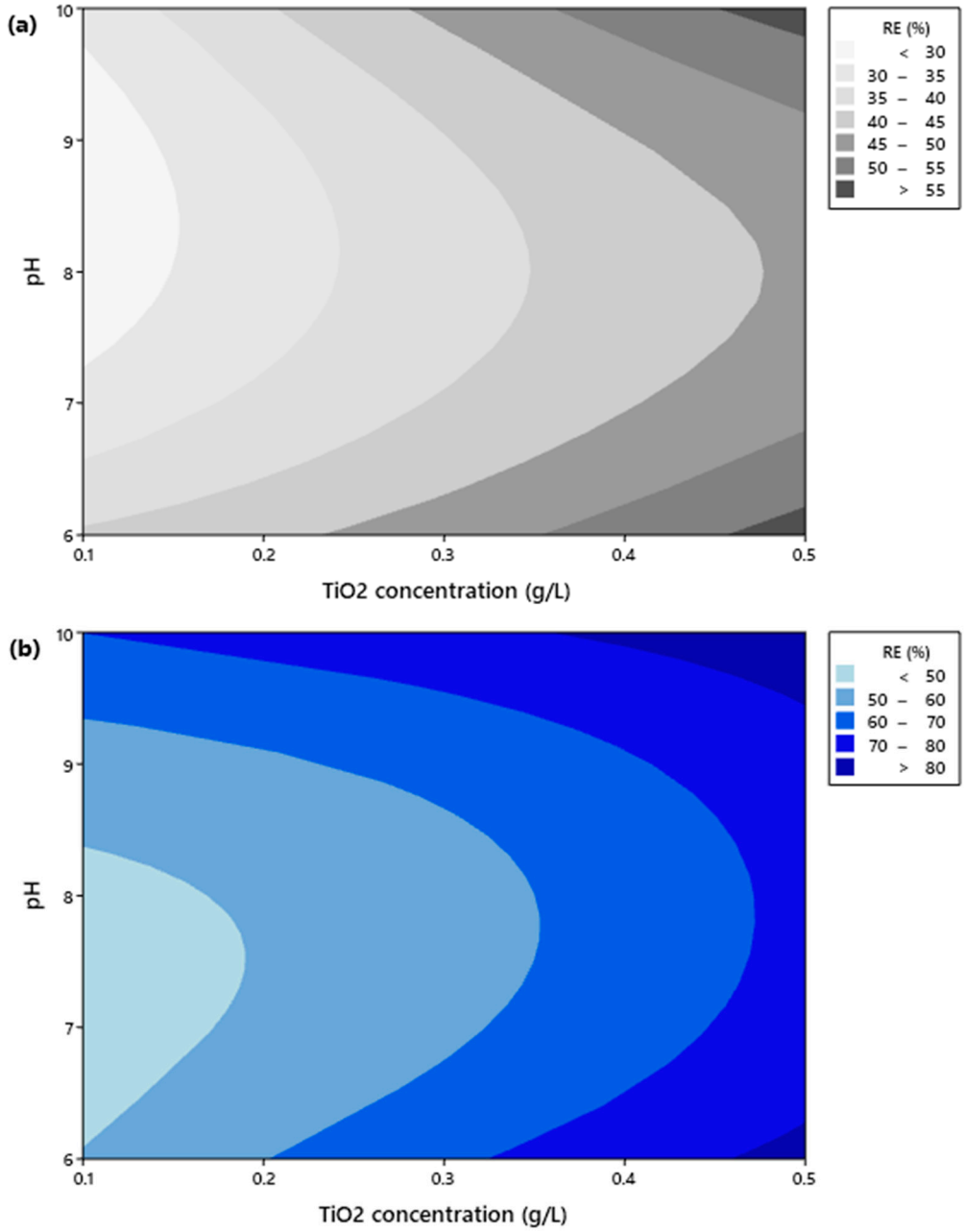

Figure 1. Removal (RE) of (**a**) protein and (**b**) carbohydrates from AOM with TiO_2/UV using different values of pH (6 to 10) and TiO_2 concentration (0.1 to 0.5 g·L^{-1}). The experiments were carried out for 2 h.

The ANOVA analysis indicated that the quadratic model was highly significant for the removal of protein (*F*-value = 86.56, $p = 0.002$) and carbohydrates (*F*-value = 103.05, $p = 0.001$). There was a close correlation between the experimental ($R^2 > 99.31\%$) and predicted values (adj. $R^2 > 98.16\%$). The lack of fit was statistically insignificant ($p > 0.05$). The second-degree polynomial equation generated by multiple regression analysis showed the significance ($p < 0.02$) of linear (TiO_2 and pH), interactive (pH × TiO_2), and quadratic (pH^2) factors in predicting protein and carbohydrate oxidation from AOM with TiO_2/UV. Meanwhile, the quadratic ($TiO_2{}^2$) terms were statistically insignificant ($p > 0.05$). The final equations for the removal of protein (Equation (2)) and carbohydrates (Equation (3)), expressed in terms of actual factor, are as follows:

$$\text{Protein removal (\%)} = 200.5 - 42.38 \times \text{pH} + 14.2 \times TiO_2 + 5.67 \times \text{pH} \times TiO_2 + 2.488 \times (\text{pH})^2 \quad (2)$$

$$\text{Carbohydrate removal (\%)} = 212.7 - 48.34 \times \text{pH} + 128.5 \times TiO_2 - 10.14 \times \text{pH} \times TiO_2 + 3.380 \times (\text{pH})^2 \quad (3)$$

The TiO_2 nanoparticles can also remove AOM via adsorption. To understand this process, adsorption experiments were completed under the same operational conditions without UV light (Figure 2a). The pH significantly influenced the adsorption of AOM with TiO_2 (Tukey test, $p < 0.05$). Furthermore, the adsorption efficiency decayed with the increase in pH, for example, the highest adsorption occurred at pH 6 (4.6% carbohydrate, 13.8% protein, and 4.26% DOC removal), while the lowest was at pH 9 (negligible amount). As can be observed, protein (0–13%) displayed more affinity to the TiO_2 surface than carbohydrates (0–4.6%).

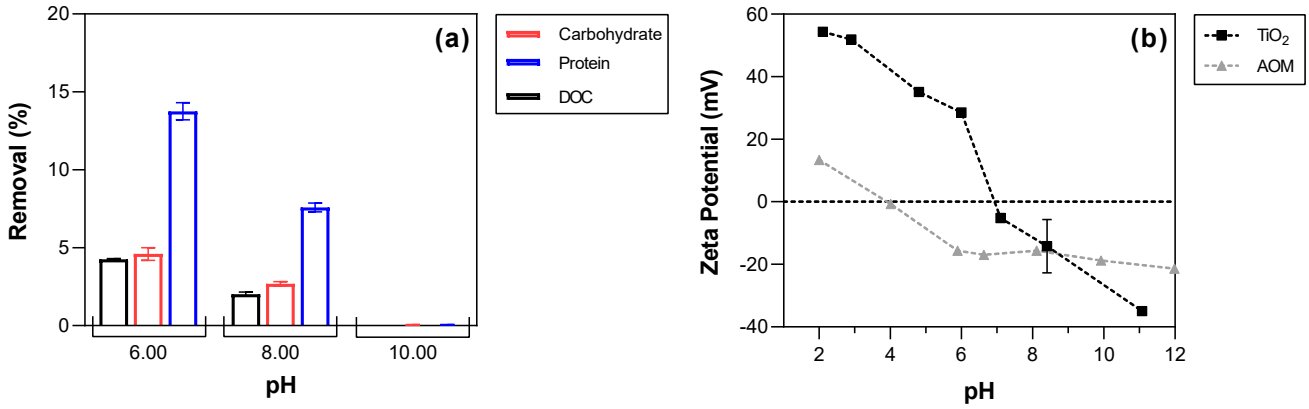

Figure 2. (**a**) AOM adsorption with TiO_2 measured in terms of protein, carbohydrate, and DOC removal. The experiments were completed under continuous agitation at 80 rpm for 2 h with 0.5 $g \cdot L^{-1}$ TiO_2 without UV light. (**b**) Zeta potential measurements of AOM and TiO_2 over pH range.

The charges involved in the process were determined over a wide pH range (Figure 2b). ZP values of AOM did not show significant variation and remained negative across the whole pH range, with the values ranging from −15.6 mV at pH 6 to −18.8 mV at pH 10, while the TiO_2 varied from 28.5 mV at pH 6 to −35 mV at pH 11. The ZP values found are in agreement with those in the literature, in which the point of zero charge of TiO_2 Degussa P25 is approximately found at pH 6.3 [35]. These differences in ZP values may explain the adsorption results (Figure 2a). The highest adsorption occurred at pH 6 when the TiO_2 (+) and AOM (−) were oppositely charged, while negligible adsorption happened at pH 10 when both were negatively charged. There may be an occurrence of repulsive electrostatic interactions between the AOM and TiO_2 at pH 10, hindering adsorption [29,32]. Li et al. (2002) [25] also reported a low adsorption of humic acid (negatively charged) with TiO_2 at a basic pH value, which was justified by repulsive interactions.

In this study, it was found that AOM removal was higher at pH 10 than at pH 6 using the same TiO_2 concentration. Domingos et al. (2009) [36] reported that maximum TiO_2 aggregation happens near the zero point of charge (pH~6.3), which reduces the mass transport rate and surface area of the TiO_2 available for adsorption/oxidation. Furthermore, acidic conditions (i.e., less OH^-) are less favorable for •OH formation via the oxidation of OH^-, reducing the attack efficiency of •OH on AOM [37]. These reasons justify the higher efficiency of TiO_2/UV at pH 10.

3.2. Response Surface of PS

The effect of the PS concentration (0.1 to 0.5 $g \cdot L^{-1}$) and pH (6 to 10) on AOM degradation with PS/UV is shown in Figure 3. Removals varied from 32.9 to 81.2% for protein (Figure 3a) and from 24.1 to 53.2% for carbohydrates (Figure 3b). The highest removals for protein (81.2%) and carbohydrates (53.2%) were obtained using a PS concentration of

0.5 g·L^{-1} at pH 8, while the lowest removals for protein (32.9%) and carbohydrates (24.1%) were found using a PS concentration of 0.1 g·L^{-1} at pH 6.

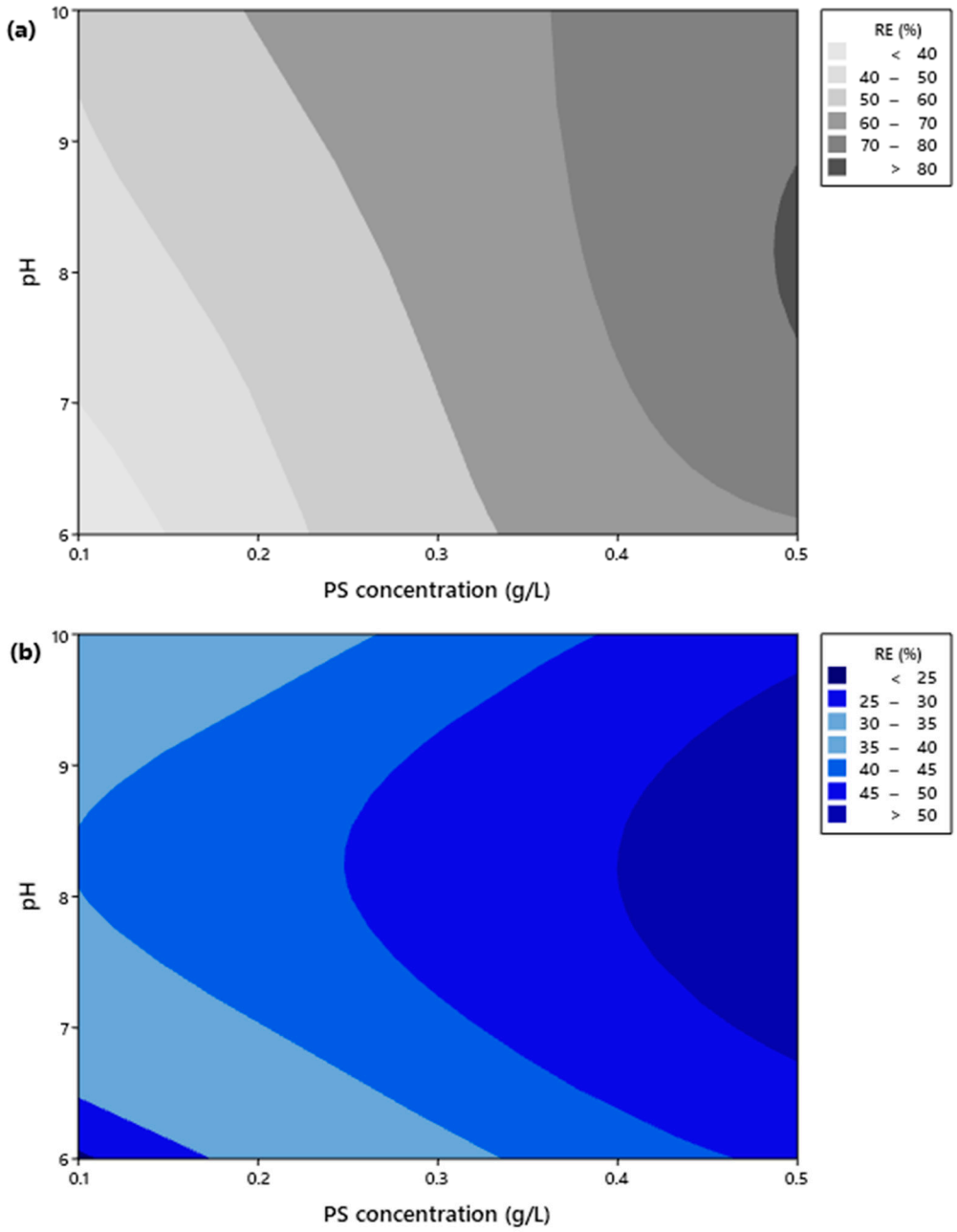

Figure 3. Removal (RE) of (**a**) protein and (**b**) carbohydrates from AOM with PS/UV using different values of pH (6 to 10) and PS concentration (0.1 to 0.5 g·L^{-1}). The experiments were carried out for 2 h.

The ANOVA analysis indicated that the quadratic model was highly significant for the removal of protein (F-value = 25.20, p = 0.012) and carbohydrates (F-value = 24.37, p = 0.012). There was a close correlation between the experimental (R^2 > 97.60%) and predicted values (adj. R^2 > 93.59%). The lack of fit was statistically insignificant (p > 0.05). The second-degree polynomial equation generated by multiple regression analysis showed the significance (p < 0.02) of linear (PS and pH), interactive (pH × PS), and quadratic (pH^2, PS^2) factors in predicting the protein and carbohydrate oxidation from AOM with PS/UV. Meanwhile, the quadratic (PS^2) term was statistically insignificant for carbohydrates (p > 0.05). The

final equations for the removal of protein (Equation (4)) and carbohydrates (Equation (5)), expressed in terms of actual factor, are as follows:

$$\text{Protein removal (\%)} = -86.3 + 207.8 \times \text{PS} + 24.6 \times \text{pH} - 9.30 \times \text{pH} \times \text{PS} - 1.198 \times (\text{pH})^2 - 9.3 \times (\text{PS})^2 \quad (4)$$

$$\text{Carbohydrate removal (\%)} = -118 + 90.3 \times \text{PS} + 35.27 \times \text{pH} - 2.9 \times \text{pH} \times \text{PS} - 2.08 \times (\text{pH})^2 \quad (5)$$

In this study, it was found that AOM removal was higher at pH 8 than at pH 6 using the same PS concentration. The •OH is the main free radical at a basic pH value, while the SO_4•$^-$ is the main species under acidic conditions [26]. This indicates that both species contribute to the maximum efficiency at pH 8 because the efficiencies are lower at pH 10 when •OH is the predominant species.

3.3. Oxidation Mechanism

The degradation of proteins and carbohydrates is caused by the radicals formed during TiO_2 (•OH and •O_2^-) and PS (•OH and SO_4•$^-$) activation using UV. The radicals, mainly comprising •OH and SO_4•$^-$, attack the protein molecules, leading to the cleavage of peptide bonds and the breakdown of amino acids [38]. This process includes the following:

$$\text{Protein} + \bullet\text{OH}/\text{SO}_4\bullet^- \rightarrow \text{peptide fragments} \quad (6)$$

$$\text{Amino acids} + \bullet\text{OH}/\text{SO}_4\bullet^- \rightarrow \text{smaller organic molecules} + \bullet\text{OH}/\text{SO}_4\bullet^- \rightarrow \text{CO}_2 + \text{H}_2\text{O} + \text{NH}_4^+ + \text{NO}_3^- \quad (7)$$

The radicals also attack carbohydrates breaking the glycosidic bonds [39]. The steps include the following:

$$\text{Carbohydrate} + \bullet\text{OH}/\text{SO}_4\bullet^- \rightarrow \text{monosaccharides} \quad (8)$$

$$\text{Monosaccharides} + \bullet\text{OH}/\text{SO}_4\bullet^- \rightarrow \text{organic acids} + \bullet\text{OH}/\text{SO}_4\bullet^- \rightarrow \text{CO}_2 + \text{H}_2\text{O} \quad (9)$$

The intermediates, such as organic acids and smaller organic molecules, continue to react with radicals until they are fully mineralized into carbon dioxide (CO_2), water (H_2O), and other inorganic ions (e.g., nitrates, ammonium ions from proteins). AOM's composition is very complex, and more details of oxidation and their sub-products cannot be provided.

3.4. Kinetics of AOM Degradation

The kinetics of AOM oxidation at different times were studied (Figure 4) using the optimal (0.5 g·L^{-1} at pH 10 for TiO_2/UV and 0.5 g·L^{-1} at pH 8 for PS/UV) and suboptimal (0.1 g·L^{-1} at pH 8 for TiO_2/UV and 0.1 g·L^{-1} at pH 6 for PS/UV) conditions. No significant increase in AOM degradation was observed after 2.0 h. Residual protein ratios (C/C_0) at 2.5 h were 0.42–0.53 and 0.19–0.33 for TiO_2/UV and PS/UV, respectively, while the carbohydrate ratios were 0.18–0.28 and 0.51–0.56, respectively.

The kinetics of AOM degradation during photocatalytic oxidation adhere to a pseudo-first-order equation (Figure 4). It is important to mention that this model neglects the AOM amount adsorbed by TiO_2 (Figure 1). Linear regression showed a great fit to the equation ($R^2 > 0.95$) for both processes. The reaction rate (k) for protein was 0.28–0.37 and 0.46–0.70 h^{-1} for TiO_2/UV and PS/UV, respectively, while the carbohydrate rates were 0.57–0.72 and 0.26–0.30 h^{-1}, respectively. A higher k value represents a higher protein/carbohydrate oxidation rate. As can be observed, the pH and the type of photocatalytic processes have significant effects on oxidation kinetics.

The PS/UV was more effective in removing protein (32.9–81.9% vs. 27.1–57.4%), while the TiO_2/UV was more effective for carbohydrate degradation (47.7–86.1% vs. 24.1–53.2%). A reason for this cannot be provided once the AOM contains different types of protein and carbohydrates with different characteristics (e.g., charge, functional groups, etc.) [40].

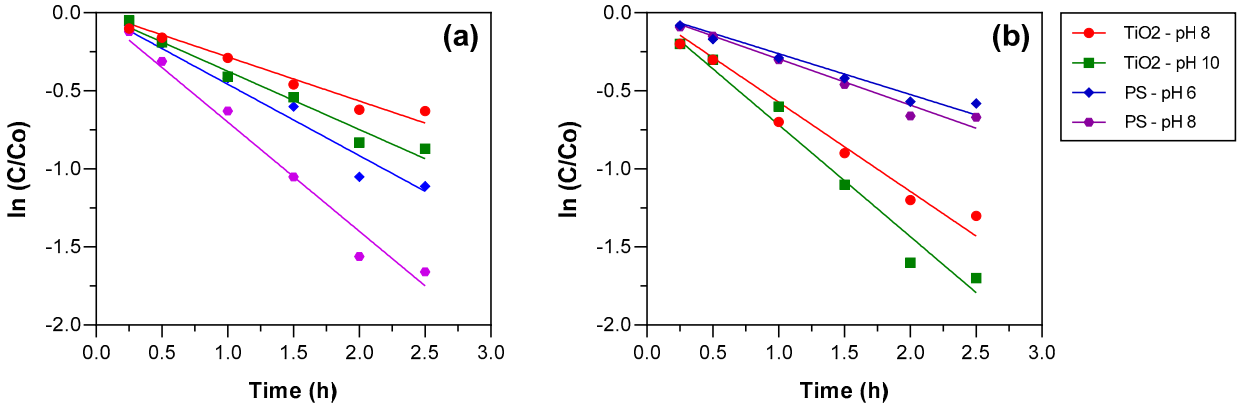

Figure 4. Kinetics of AOM degradation with TiO_2/UV and PS/UV measured by (**a**) protein and (**b**) carbohydrate analysis. The experiments were performed using 0.5 g·L^{-1} TiO_2/PS at different pH values. Predicted values using a pseudo-first-order model are shown in the continuous line.

3.5. Literature Comparison

The studies about AOM oxidation reported in the literature showed low and moderate efficiencies (0–67%) quantified by dissolved (DOC) or total (TOC) organic carbon analysis. The efficiencies follow the order of $KMnO_4$ (7.5–26%) [11] > Fe(VI) (12–24%) [19] > H_2O_2 (1.8–12.0%) [18] > peroxydisulfate (10.6%) [17] > O_3 (0–7%) [12,16]. The efficiencies increased when the two or more oxidants were applied together and follow the order of H_2O_2/Fe(VI)/UV (67.0%) [18] > H_2O_2/UV (20–50%) [21] > O_3/vacuum UV (26.7–51.1%) [24] > O_3/UV (19.9–35.6%) [24] > H_2O_2/Fe(VI) (29.8%) [18] > UV/H_2O_2/O_3 (3.5–22.5%) [23] > permonosulfate/UV (12–20%) [22]. The listed orders are derived from the results reported in multiple studies, rather than direct comparisons under identical experimental conditions. A direct comparison of our results and the ones from the literature is not possible because our results were reported in terms of protein and carbohydrate analysis. It is important to mention that protein and carbohydrates are major groups in AOM and were chosen because the sulfate from the PS/UV process can affect DOC quantification.

Based on this, UV-based technologies showed the highest removals (>50% DOC). We also reported, for the first time, promising results for protein (81.9 vs. 57.4%) and carbohydrate (53.2 vs. 86.1%) oxidation via PS/UV and TiO_2/UV, respectively. Additional research is needed to scale up both photocatalytic processes in water treatment, such as optimizing the photocatalyst configuration (UV dose), adjusting operational parameters (water flow, initial and residual oxidant concentration), configuring the immobilization surface for TiO_2, and designing efficient reactors. Pilot testing is essential to check these parameters and ensure cost-effective and energy-efficient operation at larger scales. For example, the applied UV dose (4.74–32 J·cm^{-2}) significantly exceeds the common levels used in disinfection units (0.02–0.2 J·cm^{-2}) and the scale-up of these processes would require an adjustment of the installations.

3.6. Impact on DBP Formation

The reduction in DBP formation was evaluated after the TiO_2/UV and PS/UV processes (Figure 5). Chloroform was the only THM species detected, once the bromide was not present in the AOM solution. A significant DBP reduction was found for the two photocatalytic processes (Tukey test, $p < 0.05$). The DBP formation reductions observed by TiO_2/UV—THM (84.9 to 85.6%) and CH (94.5 to 95.5%)—were similar to the efficiencies observed for PS/UV—THM (87.3 to 89.1%) and CH (82.8 to 87.5%).

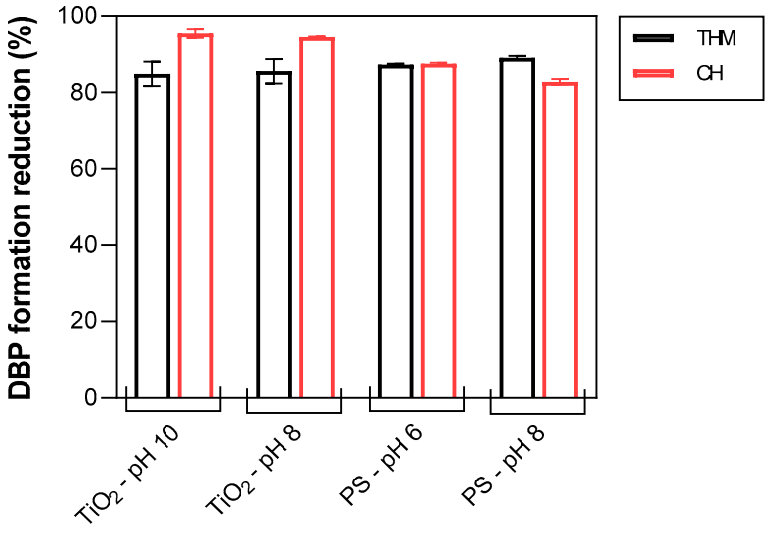

Figure 5. Reduction in disinfection by-product (DBP) formation after the application of TiO_2/UV and PS/UV. The experiments were carried out using 0.5 g·L^{-1} TiO_2/PS at different pH values for 2.5 h.

No significant differences were observed for the THM reduction between the TiO_2/UV and PS/UV conditions (Tukey test, $p < 0.05$), while significant differences were found for CH conditions between the TiO_2/UV and PS/UV conditions (Tukey test, $p < 0.05$), except for a comparison between the two TiO_2 conditions (pH 8 and 10). These results indicate that both photocatalytic processes were able to degrade the THM precursors despite the difference in the oxidation efficiency. Ma et al. (2022) [41] identified protein (88.1%) as the main precursor of chloroform formation from the intracellular organic matter chlorination of *Microcystic aeruginosa*. Considering that the PS/UV was more effective in removing protein (67–81% vs. 47–58%), it may explain how the reductions are close between the TiO_2/UV and PS/UV processes.

The reductions in THM formation found here for TiO_2/UV and PS/UV are in agreement with the results in the literature for AOM degradation by photocatalytic processes. Our previous study found a reduction of 83.4% for AOM degradation of *C. sorokiniana* by photo-Fenton [18]. However, the results are higher than the ones obtained using only UV. Chen et al. (2018) [14] decreased THM formation by 43.3–46% after the UV degradation (1.0 J·cm^{-2}) of *M. aeruginosa* AOM. On the other hand, Visentin et al. (2020) [15] found that THM formation increased by 15–20% after vacuum UV treatment (0.35 J·cm^{-2}) of water from three Canadian lakes impacted by cyanobacterial blooms. These results endorse the need to use oxidants together with UV treatment to reach better results.

There is no available literature on the reduction in CH by AOM oxidation. CH is an intermediate by-product, capable of decomposing into chloroform and trichloroacetic acid under some experiment conditions [42]. Thus, the analysis of CH degradation was difficult to conduct due to the trichloroacetic acid not being quantified in this study.

4. Conclusions

This work investigated AOM oxidation via TiO_2/UV and PS/UV. The effect of oxidant concentration (0.1 to 0.5 g·L^{-1}) and pH (6 to 10) on AOM degradation was evaluated using response surface methodology. In general, PS/UV was more effective for removing protein, while TiO_2/UV was more effective for carbohydrate degradation. TiO_2/UV removals varied from 27 to 57% for protein and from 48 to 86% for carbohydrates. The optimal condition (57% for protein and 86% for carbohydrates) was obtained using a 0.5 g·L^{-1} TiO_2 concentration at pH 10. PS/UV removals varied from 33 to 81% for protein and from 24 to 53% for carbohydrates. The optimal condition (81% for protein and 53% for carbohydrates) was obtained using a 0.5 g·L^{-1} PS concentration at pH 8. Degradation kinetics showed a good fit to the pseudo-first-order model ($R^2 > 95\%$) for both processes. The DBP formation

reductions observed via TiO_2/UV—THM (85 to 86%) and CH (94 to 96%)—were similar to the efficiencies observed for PS/UV—THM (87 to 89%) and CH (83 to 88%). These results show the efficiency of UV-based technology for AOM degradation and the control of DBP formation.

Author Contributions: L.d.S.L.: conceptualization, methodology, data curation, writing—original draft preparation, and writing—review and editing; M.T.H.: methodology and data curation; D.V.d.S.: methodology and data curation; L.A.D.: writing—review and editing, supervision, and funding acquisition. All authors have read and agreed to the published version of the manuscript.

Funding: This work was supported by the São Paulo Research Foundation (FAPESP) for a PhD scholarship [Proc. 2019/05759-1].

Data Availability Statement: Data are contained within this article.

Conflicts of Interest: The authors declare no conflicts of interest.

References

1. Zeng, G.; Zhang, R.; Liang, D.; Wang, F.; Han, Y.; Luo, Y.; Gao, P.; Wang, Q.; Wang, Q.; Yu, C.; et al. Comparison of the Advantages and Disadvantages of Algae Removal Technology and Its Development Status. *Water* **2023**, *15*, 1104. [CrossRef]
2. Griffith, A.W.; Gobler, C.J. Harmful Algal Blooms: A Climate Change Co-Stressor in Marine and Freshwater Ecosystems. *Harmful Algae* **2020**, *91*, 101590. [CrossRef] [PubMed]
3. Leite, L.D.S.; Ogura, A.P.; dos Santos, D.V.; Espíndola, E.L.G.; Daniel, L.A. Acute Toxicity of Disinfection By-Products from Chlorination of Algal Organic Matter to the Cladocerans Ceriodaphnia Silvestrii and Daphnia Similis: Influence of Bromide and Quenching Agent. *Environ. Sci. Pollut. Res.* **2022**, *29*, 35800–35810. [CrossRef] [PubMed]
4. Leite, L.D.S.; Daniel, L.A.; Bond, T. Algal Organic Matter as a Disinfection By-Product Precursor during Chlor(Am)Ination: A Critical Review. *Environ. Sci. Water Res. Technol.* **2023**, *9*, 2787–2802. [CrossRef]
5. Henderson, R.K.; Parsons, S.A.; Jefferson, B. The Impact of Differing Cell and Algogenic Organic Matter (AOM) Characteristics on the Coagulation and Flotation of Algae. *Water Res.* **2010**, *44*, 3617–3624. [CrossRef]
6. Naceradska, J.; Novotna, K.; Cermakova, L.; Cajthaml, T.; Pivokonsky, M. Investigating the Coagulation of Non-Proteinaceous Algal Organic Matter: Optimizing Coagulation Performance and Identification of Removal Mechanisms. *J. Environ. Sci.* **2019**, *79*, 25–34. [CrossRef] [PubMed]
7. Baresova, M.; Pivokonsky, M.; Novotna, K.; Naceradska, J.; Branyik, T. An Application of Cellular Organic Matter to Coagulation of Cyanobacterial Cells (Merismopedia Tenuissima). *Water Res.* **2017**, *122*, 70–77. [CrossRef] [PubMed]
8. Collins, M.R.; Eighmy, T.T.; Fenstermacher, J.M.; Spanos, S.K. Removing Natural Organic Matter by Conventional Slow Sand Filtration. *J./Am. Water Work. Assoc.* **1992**, *84*, 80–90. [CrossRef]
9. Dong, F.; Lin, Q.; Li, C.; He, G.; Deng, Y. Impacts of Pre-Oxidation on the Formation of Disinfection Byproducts from Algal Organic Matter in Subsequent Chlor(Am)Ination: A Review. *Sci. Total Environ.* **2021**, *754*, 141955. [CrossRef] [PubMed]
10. Yang, C.; Wu, H.; Cai, M.; Zhou, Y.; Guo, C.; Han, Y.; Zhang, L. Valorization of Biomass-Derived Polymers to Functional Biochar Materials for Supercapacitor Applications via Pyrolysis: Advances and Perspectives. *Polymers* **2023**, *15*, 2741. [CrossRef]
11. Naceradska, J.; Pivokonsky, M.; Pivokonska, L.; Baresova, M.; Henderson, R.K.; Zamyadi, A.; Janda, V. The Impact of Pre-Oxidation with Potassium Permanganate on Cyanobacterial Organic Matter Removal by Coagulation. *Water Res.* **2017**, *114*, 42–49. [CrossRef]
12. Novotná, K.; Pivokonský, M.; Prokopová, M.; Barešová, M.; Pivokonská, L. Consequences of Ozonation for the Limited Coagulation of Non-Proteinaceous AOM and Formation of Aldehydes as Ozonation by-Products. *J. Environ. Chem. Eng.* **2020**, *8*, 104455. [CrossRef]
13. Lin, Q.; Dong, F.; Li, C.; Cui, J. Disinfection Byproduct Formation from Algal Organic Matters after Ozonation or Ozone Combined with Activated Carbon Treatment with Subsequent Chlorination. *J. Environ. Sci.* **2021**, *104*, 233–241. [CrossRef]
14. Chen, S.; Deng, J.; Li, L.; Gao, N. Evaluation of Disinfection By-Product Formation during Chlor(Am)Ination from Algal Organic Matter after UV Irradiation. *Environ. Sci. Pollut. Res.* **2018**, *25*, 5994–6002. [CrossRef]
15. Visentin, F.; Bhartia, S.; Mohseni, M.; Peldszus, S.; Dorner, S.; Barbeau, B. Impact of Vacuum UV on Natural and Algal Organic Matter from Cyanobacterial Impacted Waters. *Environ. Sci. Water Res. Technol.* **2020**, *6*, 829–838. [CrossRef]
16. Wu, Y.; Bu, L.; Zhu, S.; Chen, F.; Li, T.; Zhou, S.; Shi, Z. Molecular Transformation of Algal Organic Matter during Sequential Ozonation-Chlorination: Role of Pre-Ozonation and Properties of Chlorinated Disinfection Byproducts. *Water Res.* **2022**, *223*, 119008. [CrossRef]
17. Yun, L.; Gao, Z.; Cheng, X.; Li, P.; Wang, L.; Guo, N.; Luo, C.; Zhu, X.; Liu, B.; Wu, D.; et al. Effect of Peroxydisulfate Oxidation Catalyzed with Ordered Mesoporous Carbons on Controlling Ultrafiltration Membrane Fouling by Algal Organic Matter. *Chemosphere* **2022**, *303*, 135037. [CrossRef]
18. Leite, L.D.S.; Silva, K.J.S.; dos Santos, D.V.; Sabogal-Paz, L.P.; Daniel, L.A. Algal Organic Matter Degradation by Chemical and Photo-Chemical Processes: A Comparative Study. *Water Air Soil Pollut.* **2022**, *233*, 457. [CrossRef]

19. Dong, F.; Lin, Q.; Li, C.; Zhang, T. Evaluation of Disinfection Byproduct Formation from Extra- And Intra-Cellular Algal Organic Matters during Chlorination after Fe(vi) Oxidation. *RSC Adv.* **2019**, *9*, 41022–41030. [CrossRef]
20. Sun, W.; Dong, H.; Wang, Y.; Duan, S.; Ji, W.; Huang, H.; Gu, J.; Qiang, Z. Ultraviolet (UV)-Based Advanced Oxidation Processes for Micropollutant Abatement in Water Treatment: Gains and Problems. *J. Environ. Chem. Eng.* **2023**, *11*, 110425. [CrossRef]
21. Zhang, X.; Fan, L.; Roddick, F.A. Effect of Feedwater Pre-Treatment Using UV/H_2O_2 for Mitigating the Fouling of a Ceramic MF Membrane Caused by Soluble Algal Organic Matter. *J. Memb. Sci.* **2015**, *493*, 683–689. [CrossRef]
22. Lee, H.; Lim, J.; Zhan, M.; Hong, S. UV-LED/PMS Preoxidation to Control Fouling Caused by Harmful Marine Algae in the UF Pretreatment of Seawater Desalination. *Desalination* **2019**, *467*, 219–228. [CrossRef]
23. Wang, X.; Wang, X.; Mi, J.; Du, Q.; Wang, Y.; Chen, W.; Sun, D.; Song, W.; Shao, M.; Jia, R. UV/H_2O_2/O_3 Removal Efficiency and Characterization of Algae-Derived Organic Matter and Odorous Substances. *J. Environ. Chem. Eng.* **2023**, *11*, 109128. [CrossRef]
24. Du, J.; Wang, C.; Zhao, Z.; Chen, R.; Zhang, P.; Cui, F. Effect of Vacuum Ultraviolet/Ozone Pretreatment on Alleviation of Ultrafiltration Membrane Fouling Caused by Algal Extracellular and Intracellular Organic Matter. *Chemosphere* **2022**, *305*, 135455. [CrossRef] [PubMed]
25. Li, X.Z.; Fan, C.M.; Sun, Y.P. Enhancement of Photocatalytic Oxidation of Humic Acid in TiO_2 Suspensions by Increasing Cation Strength. *Chemosphere* **2002**, *48*, 453–460. [CrossRef]
26. Ji, G.; Sun, S.; Jia, R.; Liu, J.; Yao, Z.; Wang, M.; Zhao, Q.; Hou, L. Study on the Removal of Humic Acid by Ultraviolet/Persulfate Advanced Oxidation Technology. *Environ. Sci. Pollut. Res.* **2020**, *27*, 26079–26090. [CrossRef]
27. Lee, J.Y.; Choi, J.H. Sonochemical Synthesis of Ce-Doped TiO_2 Nanostructure: A Visible-Light-Driven Photocatalyst for Degradation of Toluene and O-Xylene. *Materials* **2019**, *12*, 1265. [CrossRef]
28. Hoang, N.T.; Nguyen, V.T.; Minh Tuan, N.D.; Manh, T.D.; Le, P.C.; Van Tac, D.; Mwazighe, F.M. Degradation of Dyes by UV/Persulfate and Comparison with Other UV-Based Advanced Oxidation Processes: Kinetics and Role of Radicals. *Chemosphere* **2022**, *298*, 134197. [CrossRef]
29. Leite, L.D.S.; Hoffmann, M.T.; de Vicente, F.S.; dos Santos, D.V.; Daniel, L.A. Adsorption of Algal Organic Matter on Activated Carbons from Alternative Sources: Influence of Physico-Chemical Parameters. *J. Water Process Eng.* **2021**, *44*, 102435. [CrossRef]
30. Leite, L.D.S.; Daniel, L.A.; Pivokonsky, M.; Novotna, K.; Branyikova, I.; Branyik, T. Interference of Model Wastewater Components with Flocculation of Chlorella Sorokiniana Induced by Calcium Phosphate Precipitates. *Bioresour. Technol.* **2019**, *286*, 121352. [CrossRef]
31. Dubois, M.; Gilles, K.A.; Hamilton, J.K.; Rebers, P.A.; Smith, F. Colorimetric Method for Determination of Sugars and Related Substances. *Anal. Chem.* **1956**, *28*, 350–356. [CrossRef]
32. Leite, L.D.S.; Hoffmann, T.; de Vicente, F.S.; dos Santos, D.V.; Mesquita, A.; Juliato, F.B.; Daniel, L.A. Screening of New Adsorbents to Remove Algal Organic Matter from Aqueous Solutions: Kinetic Analyses and Reduction of Disinfection by-Products Formation. *Environ. Sci. Pollut. Res.* **2022**, *30*, 2800–2812. [CrossRef] [PubMed]
33. Leite, L.D.S.; dos Santos, D.V.; Paschoalato, C.F.P.R.; Bond, T.; Daniel, L.A. Disinfection By-Products Formation from Chlor(Am)Ination of Algal Organic Matter of Chlorella Sorokiniana. *Toxics* **2023**, *11*, 690. [CrossRef]
34. U.S. EPA. *Method 551.1: Determination of Chlorination Disinfection Byproducts, Chlorinated Solvents, and Halogenated Pesticides/Herbicides in Drinking Water by Liquid-Liquid Extraction and Gas Chromatography with Electron-Capture Detection*; U.S. EPA: Cincinnati, OH, USA, 1995.
35. Liao, H.; Reitberger, T. Generation of Free OHaq Radicals by Black Light Illumination of Degussa (Evonik) P25 TiO_2 Aqueous Suspensions. *Catalysts* **2013**, *3*, 418–443. [CrossRef]
36. Domingos, R.F.; Tufenkji, N.; Wilkinson, K.J. Aggregation of Titanium Dioxide Nanoparticles: Role of a Fulvic Acid. *Environ. Sci. Technol.* **2009**, *43*, 1282–1286. [CrossRef]
37. Phong, D.D.; Hur, J. Insight into Photocatalytic Degradation of Dissolved Organic Matter in UVA/TiO_2 Systems Revealed by Fluorescence EEM-PARAFAC. *Water Res.* **2015**, *87*, 119–126. [CrossRef]
38. Liu, F.; Lai, S.; Tong, H.; Lakey, P.S.J.; Shiraiwa, M.; Weller, M.G.; Pöschl, U.; Kampf, C.J. Release of Free Amino Acids upon Oxidation of Peptides and Proteins by Hydroxyl Radicals. *Anal. Bioanal. Chem.* **2017**, *409*, 2411–2420. [CrossRef] [PubMed]
39. Guay, D.F.; Cole, B.J.W.; Fort, R.C.; Genco, J.M.; Hausman, M.C. Mechanisms of Oxidative Degradation of Carbohydrates during Oxygen Delignification. I. Reaction of Methyl β-D-Glucopyranoside with Photochemically Generated Hydroxyl Radicals. *J. Wood Chem. Technol.* **2000**, *20*, 375–394. [CrossRef]
40. Safarikova, J.; Baresova, M.; Pivokonsky, M.; Kopecka, I. Influence of Peptides and Proteins Produced by Cyanobacterium Microcystis Aeruginosa on the Coagulation of Turbid Waters. *Sep. Purif. Technol.* **2013**, *118*, 49–57. [CrossRef]
41. Ma, L.; Peng, F.; Dong, Q.; Li, H.; Yang, Z. Identification of the Key Biochemical Component Contributing to Disinfection Byproducts in Chlorinating Algogenic Organic Matter. *Chemosphere* **2022**, *296*, 133998. [CrossRef]
42. Barrott, L. Chloral Hydrate: Formation and Removal by Drinking Water Treatment. *J. Water Supply Res. Technol. AQUA* **2004**, *53*, 381–390. [CrossRef]